# Yule–Nielsen based recto–verso color halftone transmittance prediction model

Mathieu Hébert[1,*] and Roger D. Hersch[2]

[1]Université de Lyon, Université Jean Monnet de Saint-Etienne, CNRS UMR5516 Laboratoire Hubert Curien,
F-42000 Saint-Etienne, France

[2]School of Computer and Communication Sciences, Ecole Polytechnique Fédérale de Lausanne (EPFL),
CH-1015 Lausanne, Switzerland

*Corresponding author: mathieu.hebert@univ-st-etienne.fr

The transmittance spectrum of halftone prints on paper is predicted thanks to a model inspired by the Yule–Nielsen modified spectral Neugebauer model used for reflectance predictions. This model is well adapted for strongly scattering printing supports and applicable to recto–verso prints. Model parameters are obtained by a few transmittance measurements of calibration patches printed on one side of the paper. The model was verified with recto–verso specimens printed by inkjet with classical and custom inks, at different halftone frequencies and on various types of paper. Predictions are as accurate as those obtained with a previously developed reflectance and transmittance prediction model relying on the multiple reflections of light between the paper and the print–air interfaces. Optimal $n$ values are smaller in transmission mode compared with the reflection model. This indicates a smaller amount of lateral light propagation in the transmission mode.   © 2011 Optical Society of America

*OCIS codes:*   100.2810, 120.7000.

## 1. Introduction

Color prediction for halftone prints has been an active subject of investigation for more than 60 years. For color management purposes, the relationship between printed colors and surface coverages of inks deposited on paper needs to be established. This is achieved by measuring the reflectance spectra of many printed patches, or by predicting them thanks to an appropriate model. For accurate prediction, the model must take into account the "optical dot gain," i.e., due to light scattering, the lateral propagation of light between the different colorant areas of the halftone [1]. Two types of models can be used. The first is based on the Yule–Nielsen equation [2,3]. In order to model the effect of optical dot gain, the halftone reflectance is given by a sum of fulltone print reflectances raised to a power $1/n$. The $n$ parameter is an empirical parameter fitted according to the considered printing technology, dithering method, paper, and inks. The second approach is based on the Clapper–Yule equation, derived from an optical model accounting for the reflectance of the paper substrate and the absorbance of the inks [4]. Recent extensions provide very good predictions for a wide range of diffusing supports and printing technologies [5].

By definition, these reflectance models apply when the light source and the observer are located on the same side of the print. But some printed objects are illuminated from behind such as advertisement light panels, neon signs, or lampshades. The prediction of the resulting colors requires a transmittance model. Recently, we developed a first reflectance and transmittance prediction model as an extension of the Clapper–Yule model, also valid for recto–verso prints [6,7]. It describes the multiple reflections of light between the paper and the print–air interfaces (Fig. 1). The angle-dependent attenuation of light within the colorants followed the approach of Williams and
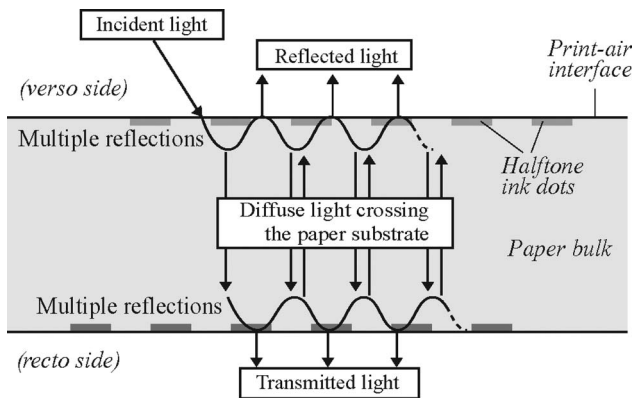
Fig. 1. Physical model of the interaction of light with a recto–verso print on paper accounting for the multiple reflections between the paper bulk and the print–air interfaces.

Clapper [8] and the spreading of the inks was accounted for according to the method proposed in [9]. The parameters used by that model were the reflectance and the transmittance of the paper substrate, the transmittance of the colorant layers, the surface coverages of the colorants, and the Fresnel coefficients corresponding to the reflection and transmission of light at the print–air interfaces. That first model illustrated the ability to extend a reflectance-only model to transmittance.

In a similar manner, we now propose as a transmittance model [10] an extension of the Yule–Nielsen modified spectral Neugebauer model [3]. In order to verify its prediction accuracy, we tested the proposed model with recto–verso halftones printed by inkjet with classical cyan, magenta, and yellow (CMY) as well as with custom inks, at different halftone frequencies and on various types of paper. Before introducing the model, let us recall that the transmittance of a diffusing layer or multilayer does not change when flipped upsidedown with respect to the light source. This property, that Kubelka called "nonpolarity of transmittance" [11], remains valid when the strongly scattering layer is coated with inks and bounded by interfaces with air, provided the geometries of illumination and of observation are identical, for example, directional illumination at 0° and observation at 0° [12]. When the two geometries are different, flipping the print may induce a small variation of its transmittance spectrum. Nonpolarity of transmittance applies for single-sided as well as for recto–verso prints. There is no equivalent in the reflectance mode.

## 2. Yule–Nielsen Model for Transmittance

A halftone is a mosaic of juxtaposed colorant areas obtained by printing the ink dot layers. The areas with no ink, those with a single ink layer, and those with two or three superposed ink layers are each considered a distinct colorant (also called Neugebauer primary). For three primary inks (e.g., cyan, magenta, and yellow), one obtains a set of eight colorants: no ink, cyan alone, magenta alone, yellow alone, red (magenta and yellow), green (cyan and yellow), blue (cyan and magenta), and black (cyan, magenta, and yellow). The paper coated with colorant $k$ on the recto side has a transmittance spectrum $T_k(\lambda)$, which can be measured with a spectrophotometer in transmittance mode, e.g. the X-Rite Color i7 instrument in total transmittance mode (d:0° geometry).

In classical clustered-dot or error diffusion prints, the fractional area occupied by each colorant can be deduced from the surface coverages of the primary inks according to Demichel's equations [13]. For cyan, magenta, and yellow primary inks with respective surface coverages $c$, $m$, and $y$, the surface coverages of the eight colorants are, respectively,

$$
\begin{aligned}
a_w &= (1-c)(1-m)(1-y), \\
a_c &= c(1-m)(1-y), \\
a_m &= (1-c)m(1-y), \\
a_y &= (1-c)(1-m)y, \\
a_{m+y} &= (1-c)my, \\
a_{c+y} &= c(1-m)y, \\
a_{c+m} &= cm(1-y), \\
a_{c+m+y} &= cmy. 
\end{aligned}
\tag{1}
$$

Let us assume, as a first approximation, that the transmittance of the halftone print is the sum of the colorant-on-paper transmittances $T_k(\lambda)$ weighted by their respective surface coverages $a_k$. We obtain a transmittance expression similar to the spectral Neugebauer reflectance model [3,14]

$$
T(\lambda) = \sum_{j=1}^{8} a_j T_j(\lambda). \tag{2}
$$

However, the linear Eq. (2) does not predict correctly the transmittance of halftone prints due to the scattering of light within the paper bulk and the multiple reflections between the paper bulk and the print–air interface, which induce lateral propagation of light from one colorant area to another. This phenomenon, known for reflectance as the "Yule–Nielsen effect" [3,15], also occurs in the transmittance mode (see Fig. 1). In order to account for this effect, we follow the same approach as Viggiano [3] by raising all the transmittances in Eq. (2) to a power of $1/n$. We obtain the Yule–Nielsen modified Neugebauer equation for the transmittance of a color halftone printed on the recto side:

$$
T(\lambda) = \left[ \sum_{j=1}^{8} a_j T_j^{1/n}(\lambda) \right]^n. \tag{3}
$$

A second phenomenon well known in halftone printing is the spreading of inks on the paper and on the other inks [9]. In order to obtain accurate spectral transmittance predictions, effective surface

coverages need to be known. They are deduced from the measured transmittance spectra of a selection of printed halftones, called calibration patches.

## 3. Effective Surface Coverages

The amount of ink spreading is different for each ink and depends on whether the ink is alone on paper or superposed with other inks. Effective surface coverages are therefore computed for all ink superposition combinations. Each ink is printed at 0.25, 0.5, and 0.75 nominal surface coverage, (a) alone on paper, (b) superposed to a solid layer of a second ink, (c) superposed to a solid layer of the third ink, and (d) superposed to a solid layer of the second and third inks. In total, for 3 inks, there are 12 different superposition conditions $(3 + 2 \times 3 + 3)$. With three halftones per superposition condition, 36 calibration patches are printed. The effective surface coverage $q_{i/j}$ of ink halftone $i$ superposed with solid colorant $j$ is fitted by minimizing the sum of square differences between the transmittance predicted by Eq. (3)

$$P(\lambda) = [(1-x)T_j^{1/n}(\lambda) + xT_{i\&j}^{1/n}(\lambda)]^n$$

and the measured transmittance $M(\lambda)$:

$$q_{i/j} = \underset{0 \leq x \leq 1}{\mathrm{argmin}} \sum_{\lambda=380\,\mathrm{nm}}^{730\,\mathrm{nm}} [M(\lambda) - P(\lambda)]^2, \qquad (4)$$

where $T_j$ and $T_{i\&j}$ denote the colorant-on-paper transmittances for, respectively, the solid colorant $j$ (which may be the unprinted paper) and the superposition of solid ink $i$ and solid colorant $j$. We assume that the effective surface coverage is 0, respectively 1, when the nominal surface coverage is 0 (no ink), respectively 1 (full coverage). We obtain a list of effective surface coverages $q_{i/j}$, which by linear interpolation yields a continuous curve $q_{i/j} = f_{i/j}(q_0)$, where $q_0$ is the nominal ink surface coverage (Fig. 2).

The ink spreading curves are established from patches where only one ink is halftoned. Let us now consider that the three inks, cyan, magenta,
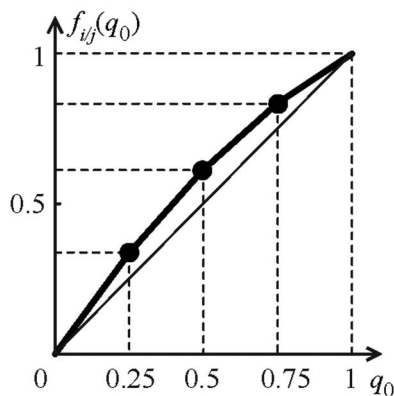


Fig. 2. Example of ink spreading curve, giving the effective surface coverage of ink $i$ when superposed on colorant $j$ as a function of the nominal surface coverage $q_0$.

and yellow, are halftoned, with the respective nominal surface coverages $c_0$, $m_0$, and $y_0$. Before being able to use Demichel's Eqs. (1) to calculate the effective surface coverages of the eight colorants, we need to compute the effective surface coverages $c$, $m$, $y$ of the inks, accounting for the superposition-dependent ink spreading. Effective surface coverages of an ink halftone are obtained by a weighted average of the ink spreading curves. The weights are expressed by the surface coverages of the colorants on which the ink halftone is superposed. For example, the weight of the ink spreading curve $f_c$ (cyan halftone over white colorant) is $(1-m)(1-y)$. In the case of three halftoned inks, effective surface coverages are obtained by performing a few iterations with the following equations:

$$\begin{aligned} c &= (1-m)(1-y)f_c(c_0) + m(1-y)f_{c/m}(c_0) \\ &\quad + (1-m)yf_{c/y}(c_0) + myf_{c/m+y}(c_0), \\ m &= (1-c)(1-y)f_m(m_0) + c(1-y)f_{m/c}(m_0) \\ &\quad + (1-c)yf_{m/y}(m_0) + cyf_{m/c+y}(m_0), \\ y &= (1-c)(1-m)f_y(y_0) + c(1-m)f_{y/c}(y_0) \\ &\quad + (1-c)mf_{y/m}(y_0) + cmf_{y/c+m}(y_0). \end{aligned} \qquad (5)$$

For the first iteration, $c = c_0$, $m = m_0$, and $y = y_0$ are taken as initial values on the right-hand side of the equations. The obtained values of $c$, $m$, and $y$ are then inserted again on the right-hand side of the equations. This yields new values of $c$, $m$, $y$, and so on, until the values of $c$, $m$, and $y$ stabilize. The effective surface coverages of the colorants are calculated by plugging the obtained effective surface coverages values $c$, $m$, and $y$ into Eq. (1). Then, the transmittance of the halftone patch is given by Eq. (3). Several $n$ values can be tried in order to select the one that provides the best predictions for a set of patches whose transmittance spectra have been measured.

With three ink halftones, the calibration of the model requires eight fulltone colorants (including the paper white) and either 36 or 12 patches to establish the 12 ink spreading curves, with, in each superposition condition, halftones at 0.25, 0.5, 0.75, or only at 0.5 nominal surface coverage.

## 4. Recto–Verso Halftone Prints

A recto–verso print is a paper printed on its two faces, possibly with different inks. When printed with three inks on each face, the print contains eight recto colorants (labeled $u$) and eight verso colorants (labeled $v$); therefore, 64 recto–verso colorants ($uv$). In order to obtain their transmittances $T_{uv}(\lambda)$ by measurement, the 64 recto–verso colorants need to be printed as uniform patches.

Since the paper is strongly scattering, we may assume that the lateral propagation of the light crossing the paper substrate is large compared to the halftone screen period. Hence, there is no correlation between the colorants traversed by the light at the

recto and verso sides. The probability for light to cross the recto colorant $u$ and the verso colorant $v$ is simply the product of their respective surface coverages, i.e., $a_u a_v$.

The effective colorant surface coverages $a_u$ and $a_v$ are determined separately for the recto and verso colorants. They are deduced from recto only, respectively, verso only, calibration patches according to the method presented in the previous section (e.g., in the case of three ink halftones with 20 patches on each side). In order to account for the Yule–Nielsen effect, all the transmittances are raised to the power of $1/n$. The transmittance of the recto–verso halftone print is given by

$$T(\lambda) = \left[ \sum_{u=1}^{8} \sum_{v=1}^{8} a_u a_v T_{uv}^{1/n}(\lambda) \right]^n. \qquad (6)$$

In order to reduce the number of colorant-on-paper transmittances to measure, we propose a variant of this model where only one-sided patches are needed: eight recto-only colorants and eight verso-only colorants. Each recto and verso colorant (generically labeled $j$) is characterized by an intrinsic transmittance $t_j(\lambda)$ defined as the ratio of the measured colorant-on-paper transmittance $T_j(\lambda)$ to the unprinted paper transmittance $T_p(\lambda)$:

$$t_j(\lambda) = T_j(\lambda)/T_p(\lambda). \qquad (7)$$

The recto–verso colorant-on-paper transmittances $T_{uv}(\lambda)$ are

$$T_{uv}(\lambda) = T_p(\lambda) t_u(\lambda) t_v(\lambda) \qquad (8)$$

and Eq. (6) becomes

$$T(\lambda) = T_p(\lambda) \left[ \sum_u a_u t_u^{1/n}(\lambda) \right]^n \left[ \sum_v a_v t_v^{1/n}(\lambda) \right]^n. \qquad (9)$$

Note that all the measurements and predictions should rely on the same measuring geometry and the same position for the recto face with respect to the light source. If the print is flipped, i.e., the verso face takes the place of the recto face, its transmittance may be modified especially when the light source and the capturing device have different angular geometries [6].

## 5. Verification of the Model

In order to verify the prediction model, we performed experiments based on different sets of halftone patches printed with the Canon PixmaPro 9500 inkjet printer, using various inks and papers. The halftones were designed using Adobe Photoshop. A classical clustered dot screen was used for each ink layer, with an angle of 30° between the dot screens. Different screen frequencies were tested. These dot screens were printed without subsequent dithering or tone correction.

For each ink set and paper, the spectral predictions obtained from the proposed model were compared to spectral measurements carried out with the X-Rite Color i7 spectrophotometer in total transmittance mode (verso illuminated with diffuse light and recto observed at 0°). The selected comparison metric was CIELAB $\Delta E_{94}$, obtained by converting the predicted and measured spectra first into CIE-$XYZ$ tristimulus values, calculated with a D65 illuminant and with respect to a 2° standard observer, and then into CIELAB color coordinates using as white reference the transmittance spectrum of the unprinted paper illuminated with the D65 illuminant [16].

We designed two sets of recto–verso halftones. The first set (Set A) contains 1875 patches corresponding to 125 CMY colors on the recto (cyan, magenta, and yellow inks at the nominal surface coverages 0, 0.25, 0.50, 0.75, and 1) and 15 CMY colors on the verso. The recto-only and verso-only calibration patches are contained in this set. The second set (Set B) is shown in Fig. 3. It was printed with cyan, magenta, and yellow inks on the recto side (CMY halftones), and red and green custom inks on the verso side (RG halftones). It contains the 20 recto-only calibration patches for the three-ink recto halftones, the eight
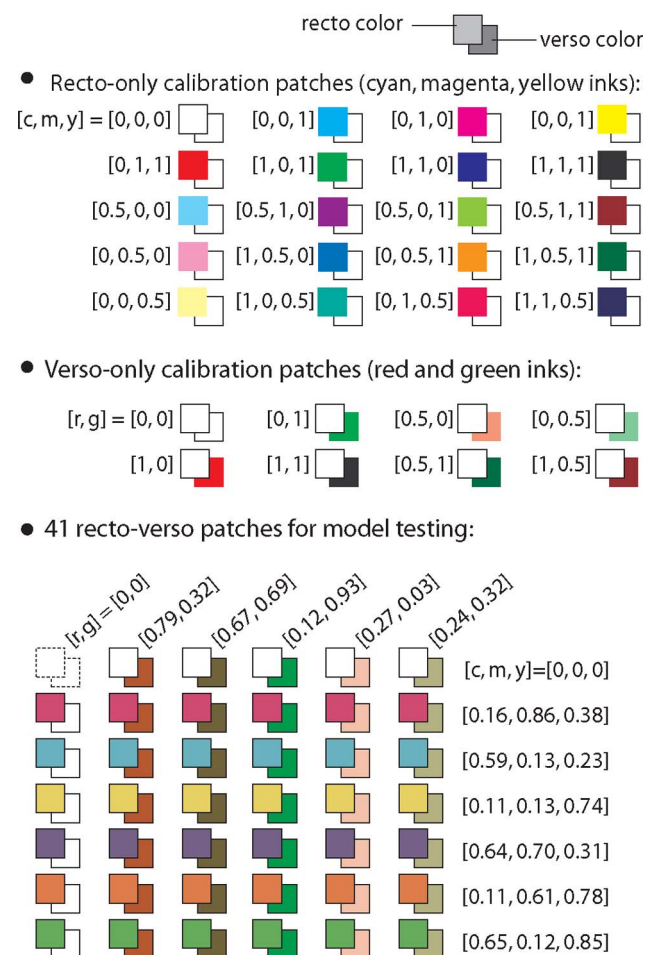


Fig. 3. (Color online) Set B of patches printed with cyan, magenta, yellow inks on the recto side, and red and green inks on the verso side.

verso-only calibration patches for the two-ink verso halftones, as well as 41 recto–verso test patches for the verification of the model: six recto-only CMY colors, five verso-only RG colors, and the 30 combinations of these six recto halftones and five verso halftones. The following papers have been tested: "APCO" is a supercalendered and nonfluorescent paper from Scheufelen Company, Germany; "Biotop" is a nonfluorescent, noncalendered paper being noticeably porous; "office" is a classical $80 \, \mathrm{g/m^2}$ paper for copy printers; and "tracing" is the $90 \, \mathrm{g/m^2}$ Canson tracing paper. Their transmittance between 550 and 600 nm gives an idea of their opacity: it is nearly 0.11 for the APCO paper, 0.19 for the Biotop paper, 0.16 for the office paper, and 0.74 for the tracing paper. The tracing paper is much more translucent than the other papers.

The first experiment aims at checking the prediction accuracy for classical CMY colors. We printed the set of 1875 of CMY recto–verso patches (Set A) on APCO paper at 120 lpi. The proposed Yule–Nielsen model extended to transmittance provides excellent predictions since the average CIELAB $\Delta E_{94}$ value over the 1875 patches is 0.98. Its prediction accuracy is comparable to one of the previously proposed reflectance and transmittance model inspired by the Clapper–Yule multiple reflection model [7] (see Table 1).

For the second experiment, we vary the halftone frequency. We printed on APCO paper the set of 41 CMY/RG patches (Set B) with 60, 90, 120, and 150 lpi screens. In a similar manner as in the reflectance mode [9], the optimal $n$ value increases as the halftone frequency increases. Expectedly, the Yule–Nielsen approach provides better predictions at 60 lpi than the multiple reflection model where the optical dot gain is modeled by assuming a high halftone frequency. Since the two sides of the paper can also be printed with different halftone frequencies, we tested the extreme case where the CMY colors on the recto are printed at 60 lpi, and the RG colors on the verso are printed at 150 lpi (see the line referred to as 60/150 lpi in Table 1). Both the Yule–

Nielsen model and the multiple reflection model provide excellent predictions.

The third experiment investigates the influence of the printing support. The Set B of patches, shown in Fig. 3, was printed at 120 lpi on APCO, Biotop, office, and tracing papers. With respect to the highly scattering and nonporous APCO paper, both the Yule–Nielsen and the multiple reflection models provide good predictions. For the office, Biotop, and tracing papers, however, the Yule–Nielsen model is noticeably less accurate than the multiple reflection model. The difference between the two models may have a mathematical origin, actually difficult to identify. But the very high $n$ value found for optimal predictions (the average color different between predictions and measurement decreases asymptotically when increasing the $n$ value, limited to 100 in our experiment) is the sign of the bad adequacy of the Yule–Nielsen model with the considered printing supports, either because the ink penetration depth is too important (office and Biotop papers) or because the scattering power is too low (tracing paper).

## 6. Model with Two Different Recto and Verso $n$ Values

In Eq. (9), the right-hand expression contains two bracketed terms containing the parameters relative to the recto halftone (first term) and those relative to the verso halftone (second term). The same $n$ value appears in both terms. It would be easy to consider different $n$ values for the recto and verso halftones, i.e., a value $n_u$ in the first bracketed term and a value $n_v$ in the second term. This would give a model with two $n$ values expressed as

$$T(\lambda) = T_p(\lambda)\left[\sum_u a_u t_u^{1/n_u}(\lambda)\right]^{n_u}\left[\sum_v a_v t_v^{1/n_v}(\lambda)\right]^{n_v}. \quad (10)$$

The model with two $n$ values may look judicious in cases where the optical dot gain is stronger on one side of the paper, for example, when a face is printed at a higher halftone frequency. Let us consider the set of 41 patches printed at 60 lpi on the recto (CMY colors) and 150 lpi on the verso (RG colors). The model with single $n$, expressed by Eq. (9), gives an average

Table 1. Average Color Difference Between Measured and Predicted Transmission Spectra

| Set of Patches | Paper | Frequency (lpi) | $n$ Value | Yule–Nielsen Transmittance Model[a] | Multiple Reflection Model[a] |
|---|---|---|---|---|---|
| 1875 CMY/CMY | APCO | 120 | 3.5 | 0.98 *(1.9)* | 1.04 *(2.1)* |
| 41 CMY/RG | APCO | 60 | 1.7 | 0.63 *(1.1)* | 0.86 *(1.7)* |
| | | 90 | 2.2 | 0.91 *(1.4)* | 0.79 *(1.4)* |
| | | 120 | 2.7 | 1.04 *(1.8)* | 1.02 *(1.6)* |
| | | 150 | 4.5 | 1.05 *(1.9)* | 0.87 *(1.3)* |
| | | 60/150[b] | 2.6 | 0.60 *(1.2)* | 0.53 *(1.0)* |
| | office | 120 | 100 | 1.09 *(2.0)* | 0.60 *(1.1)* |
| | Biotop | 120 | 100 | 1.39 *(2.7)* | 1.23 *(2.2)* |
| | tracing | 75 | 100 | 1.13 *(2.3)* | 0.63 *(1.2)* |
| | | 120 | 100 | 1.58 *(3.3)* | 1.06 *(2.1)* |

[a]Average CIELAB $\Delta E_{94}$ (95-quantile).
[b]Cyan, magenta, yellow inks printed at 60 lpi on the recto side; red and green inks printed at 150 lpi on the verso side.

$\Delta E_{94}$ of 0.60 for $n = 2.6$. The model with two $n$ values, expressed by Eq. (10), gains slightly in accuracy. The average $\Delta E_{94}$ is 0.56 for $n_u = 2.4$ and $n_v = 3.7$. It is interesting to observe that the highest $n$ value, i.e. $n_v$, is attached to the side printed with the highest halftone frequency. This confirms the fact that the optical dot gain effect, modeled by the $n$ value, becomes stronger when the halftone frequency increases.

For all the printed samples where the recto and verso halftones are printed at the same frequency, the model with two $n$ values gives nearly the same prediction results as the model with a single $n$.

## 7. Yule–Nielsen Modified Neugebauer Model in Reflection and Transmission Modes

Two versions of the Yule–Nielsen modified Neugebauer spectral prediction model are now available: one in reflection mode (classical model) and one in transmission mode. The reflectance and transmittance models are calibrated separately from reflectance, respectively, transmittance, measured spectra. Consequently, the ink spreading curves and the optimal $n$ value are different in the two models even when the same set of calibration patches is used. This is illustrated by the following experiment.

We printed 125 CMY recto-only colors (cyan, magenta, and yellow inks at the nominal surface coverages 0, 0.25, 0.50, 0.75, and 1) on one face of the APCO paper with an inkjet printer at 120 lpi. Their reflectance and transmittance spectra were measured with the X-Rite Color i7 spectrophotometer. In reflectance mode, we selected the d:8i measuring geometry: the printed side was illuminated by Lambertian light and observed at 8° with the specular component included. In transmittance mode, we selected the d:0 geometry: the unprinted side was illuminated by Lambertian light and the printed side was observed at 0°. Since the print is a quasi-Lambertian diffuser, there is no significant difference between observations at 0° and 8°.

The average color difference between predictions and measurements over the 125 colors, as well as the 95-quantiles, are given in Table 2. The $n$ value providing the best predictions is much higher in the reflectance model than in the transmittance model. This means that the lateral propagation of light between different areas in the halftone is larger for the reflected light compared with the transmitted light. Photons contributing to light reflection are on
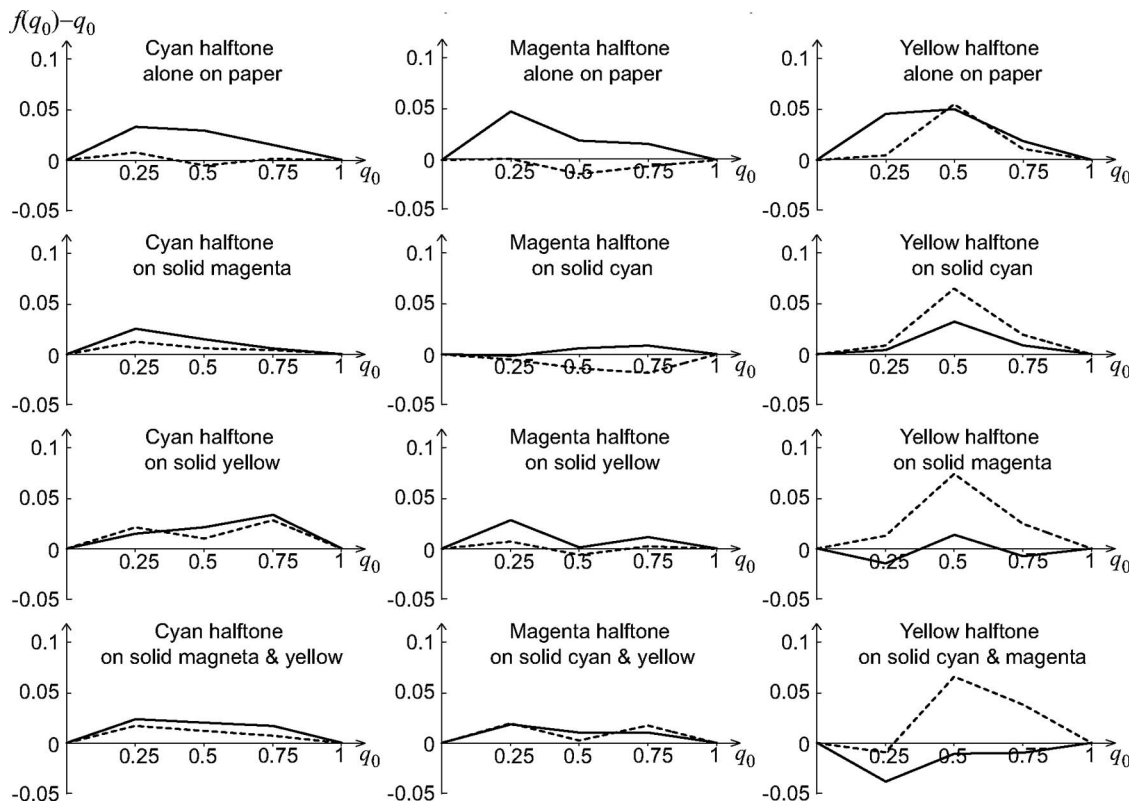


Fig. 4. Dot gain curves (difference between effective and nominal ink coverages as a function of the nominal ink coverage for a single halftoned ink) calibrated in reflectance mode (dashed lines) and transmittance mode (continuous lines). The 12 graphs correspond to cyan, magenta, or yellow halftones printed either alone on paper or superposed with a solid ink layer composed of the second ink, the third ink, or the second and third inks.

average subject to more scattering events and therefore show a stronger lateral propagation, compared with transmitted photons which do not necessarily need to strongly change their orientation.

The ink spreading curves computed when calibrating the two models are different, but their shape has some resemblance mainly with respect to the change of slope at successive nominal surface coverages. This can be seen in Fig. 4 where we plotted the dot gain curves, which correspond to the difference $f(q_0) - q_0$ between the effective surface coverage $f(q_0)$ and the nominal surface coverage $q_0$. We expected a smaller difference between the reflectance and the transmittance models since ink spreading is a mechanical effect independent of the measuring geometry. However, it is known that the ink spreading curves also compensate for additional optical phenomena, such as light scattering in the inks, especially in the ink sublayers penetrating the paper.

## 8. Conclusion

This study shows that the Yule–Nielsen modified Neugebauer model, widely used for spectral reflectance prediction, can be transposed for spectral transmittance predictions in a relatively straightforward manner. Except for the fact that colorant transmittances are used in place of colorant reflectances, the model relies on the same concept: an empirical $n$ value, applied as a $1/n$ exponent on each colorant transmittance, models the transfer of light between colorants due to the lateral propagation of the light scattered by the paper and the multiple internal reflections between the paper bulk and the print–air interface. Effective surface coverages are fitted from the transmittance of selected printed single-sided patches to account for ink spreading in each ink superposition condition. For recto–verso halftone prints, the parameters relative to the inks, i.e. the transmittance and the surface coverage of the colorants, are deduced from recto-only and verso-only printed calibration patches. Then, every recto–verso halftone combination can be predicted. The tests carried out on inkjet recto–verso prints show the excellent accuracy of the proposed Yule–Nielsen based transmittance model, especially at low halftone frequencies. Even though it is slightly less accurate than the previously proposed Clapper–Yule inspired transmittance model [7] for high halftone frequencies and highly ink-absorbing papers, it has the benefit of simplicity and of a reduced number of parameters. It also offers the possibility to use different $n$ values for the recto and verso sides, which is an advantage when the characteristics of the halftones printed on each side are different. Comparison of the optimal $n$ values in, respectively, the reflection and transmission modes shows a stronger lateral light propagation in the reflectance mode, compared with the transmission mode where the photon trajectory orientation is not reversed.

## References

1. R. D. Hersch and M. Hébert, "Interaction between light, paper and color halftones: challenges and modelization approaches," in *Proceedings of the Third European Conference on Color in Graphics, Imaging and Vision (CGIV)* (Society for Imaging Science and Technology, 2006), pp. 1–7.
2. J. A. C. Yule and W. J. Nielsen, "The penetration of light into paper and its effect on halftone reproduction," Proc. TAGA **3**, 65–76 (1951).
3. J. A. S. Viggiano, "The color of halftone tints," Proc. TAGA **37**, 647–661 (1985).
4. F. R. Clapper and J. A. C. Yule, "The effect of multiple internal reflections on the densities of halftone prints on paper," J. Opt. Soc. Am. **43**, 600–603 (1953).
5. R. D. Hersch, P. Emmel, F. Collaud, and F. Crété, "Spectral reflection and dot surface prediction models for color halftone prints," J. Electron. Imaging **14**, 033001 (2005).
6. M. Hébert and R. D. Hersch, "Reflectance and transmittance model for recto-verso halftone prints," J. Opt. Soc. Am. A **23**, 2415–2432 (2006).
7. M. Hébert and R. D. Hersch, "Reflectance and transmittance model for recto-verso halftone prints: spectral predictions with multi-ink halftones," J. Opt. Soc. Am. A **26**, 356–364 (2009).
8. F. C. Williams and F. R. Clapper, "Multiple internal reflections in photographic color prints," J. Opt. Soc. Am. **43**, 595–597 (1953).
9. R. D. Hersch and F. Crété, "Improving the Yule-Nielsen modified spectral Neugebauer model by dot surface coverages depending on the ink superposition conditions," Proc. SPIE **5667**, 434–445 (2005).
10. M. Hébert and R. D. Hersch, "Yule–Nielsen approach for predicting the spectral transmittance of halftone prints," in *Proceedings of the IS&T/SID 17th Conference on Color Imaging* (Society for Imaging Science and Technology, 2009), pp. 155–158.
11. P. Kubelka, "New contributions to the optics of intensely light-scattering materials. Part II: Nonhomogeneous layers," J. Opt. Soc. Am. **44**, 330–334 (1954).
12. M. Hébert, R. Hersch, and J. -M. Becker, "Compositional reflectance and transmittance model for multilayer specimens," J. Opt. Soc. Am. A **24**, 2628–2644 (2007).
13. M. E. Demichel, Procédés **26**, 17–21 (1924).
14. H. E. J. Neugebauer, "Die theoretischen Grundlagen des Mehrfarbendrucks," Zeitschrift fuer wissenschaftliche Photographie **36**, 36–73 (1937) ["The theoretical basis of multicolour letterpress printing," Color Res. Appl. **30**, 322–331 (2005) (in English)].
15. F. R. Ruckdeschel and O. G. Hauser, "Yule–Nielsen effect in printing: a physical analysis," Appl. Opt. **17**, 3376–3383 (1978).
16. G. Sharma, *Digital Color Imaging Handbook* (CRC Press, 2003), pp. 30–36.